Monthly Weather Review

Evaluating NAM and WRF Forecasts of Mesoscale Convective Vortices

Autumn D. Losey, Andrew T. Ryan, and Daniel E. Stewart
School of Meteorology, University of Oklahoma, Norman, Oklahoma

Adam J. Clark
National Severe Storms Laboratory, University of Oklahoma, Norman, Oklahoma

ABSTRACT

The authors perform a statistical analysis of mesoscale convective vortices (MCVs) as forecasted by the North American Model (NAM) and a version of the Weather Research and Forecasting (WRF) model run by the National Severe Storms Laboratory. Seven vortices that met specified conditions and limitations in both intensity, location, and date were selected to be studied. These storms generally occurred over the eastern half of the United States, and covered a wide range of intensities and lifespans.

Prediction of mesoscale vortices by the NAM and WRF were examined in terms of MCV intensity, duration, and path distance. In general, the NAM was more skilled at forecasting MCVs than the WRF in all of the considered variables.

1. Introduction

Mesoscale convective vortices (MCVs) are diabatically induced, mid-tropospheric circulations that form within mesoscale convective systems, that can subsist beyond the "parent" convective system, and can even lead to the formation of new mesoscale storm systems (Clark et al 2010). They form out of deep convection due to diabatic heating combined with local vorticity maximas, as found by Hertenstein and Schubert (1999). After formation, the storms maintain themselves through quasi-balanced vertical motions and the diabatic effects of moist convection. Latent heat release, evaporation, melting of precipitation, and thermal radiation also contribute to the generation of positive potential vorticity (Raymond and Jiang 1990; Markowski and Richardson 2010). Thus, while MCVs are vulnerable to large-scale vertical shear and deformation, lower amounts of shear induce further low-level lifting, allowing for continued intensification, and it has been shown that strongly sheared environments can support long-lived MCVs as well (Trier et al 2000a; Davies et al 2003). Typically forming during late spring and early summer, MCVs can cause widespread, potentially heavy rainfall that can produce localized flash flooding. They are also capable of producing localized severe weather, such as strong winds, hail, and even tornadoes (Snook 2011).

On radar, MCVs are generally visible as tight circulations, in extreme cases resembling miniature land-based hurricanes with eye-like features, an aspect that has led some historical cases [such as the 2009 (Coniglio et al. 2011) and 1980 MCVs that affected Missouri and Illinois, respectively] to be informally referred to by the public as "inland hurricanes."

Many studies have been conducted concerning mechanics and model prediction skill of mesoscale convective vortices (MCVs). In particular, this study builds off of Davis et al (2003) and their investigation of the Rapid Update Cycle (RUC)'s ability to predict various mid-tropospheric vortices, focusing on MCVs. In Davis et al. (2003) it was found that the RUC is poor at predicting MCV formation and subsequent evolution. However, when the MCV was present prior to the model initialization, the RUC model had much more skill in forecasting the track and evolution. Furthermore,

Davis et al. (2003) determined that the RUC analyses adequately depicted observed MCV location and vertical structure. Thus, RUC analyses are used herein to verify the WRF and NAM model forecasts.

Although much has been done with individual models, little research has been conducted concerning the effectiveness of many numerical models in forecasting MCV formation (Davis et al 2003) and intensity (Zhang et al 2006). (For clarification, when this study mentions "MCV intensity", it refers to the magnitude of the absolute vorticity of the MCV.) In general, most studies conclude that models can usually predict an MCV's overall track once it has been recognized. In fact, Trier et al (2000b) found that MCVs are generally predictable when it comes to track after formation due to their coherent and nondispersive structure. However, the models' lack of skill at predicting either initiation or intensity compels forecasters to utilize other methods of determining if or when an MCV will form, and whether or

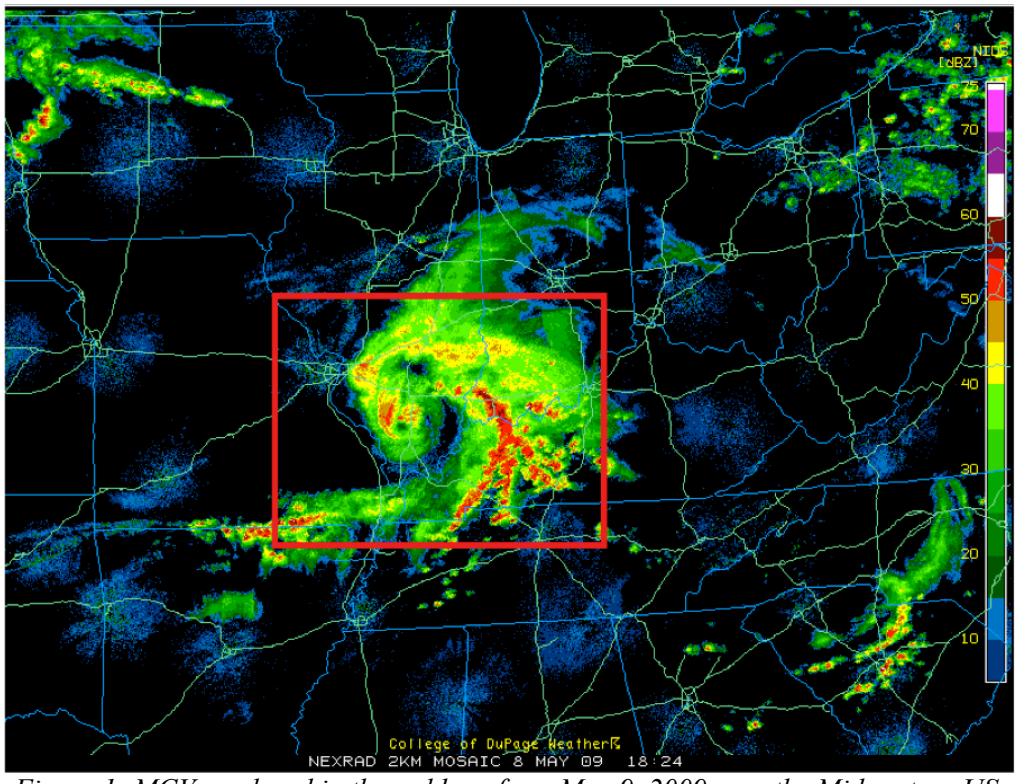

Figure 1: MCV, enclosed in the red box, from May 9, 2009 over the Midwestern US.

not it will produce severe weather. It should be noted that several studies (e.g. Bartels and Maddox 1991, Davis et al 2003) found little to no correlation between the propensity of the MCV to produce severe

weather and the size or intensity of the MCV.

It is the purpose of this study to examine two weather numerical prediction models — the North American Model (NAM) and the National Severe Storms Laboratory (NSSL) Weather Research and Forecasting (WRF) model.

2. Methods

a. Determining MCV Cases

MCV events were identified visually using the radar and satellite archive kept by the University Corporation for Atmospheric Research (UCAR). The authors selected initial cases based on visual evidence of cyclonic circulation in either radar reflectivity or visual/infrared satellite imagery, as shown in Figure 2a. If circulation was found in one platform, the other platform as well as alternative archived information [i.e. upper air charts from the Storm Prediction Center (SPC)] was used to confirm its presence.

Bartels and Maddox (1991) and later Trier et al (2000a) found that not all MCVs were not associated with large or obvious parent MCSs. As such, in defining MCVs, we did not have any requirements on parent storm size. There were also no such restrictions on MCV size.

Still, some limitations had to be considered; only the years 2007 through 2011 could be considered, further limited to only the months of May, April, and June. This time range was chosen to encapsulate the most common times of MCV formation, as well as to better incorporate the available model data. The cases also had to stay within the model's projection range. Other limitations include only selecting MCVs that persist well past their parent MCS, which ensures that a clear MCV exists for the models to capture.

Also, only regions east of the Rocky Mountains are considered, as MCVs have a climatological

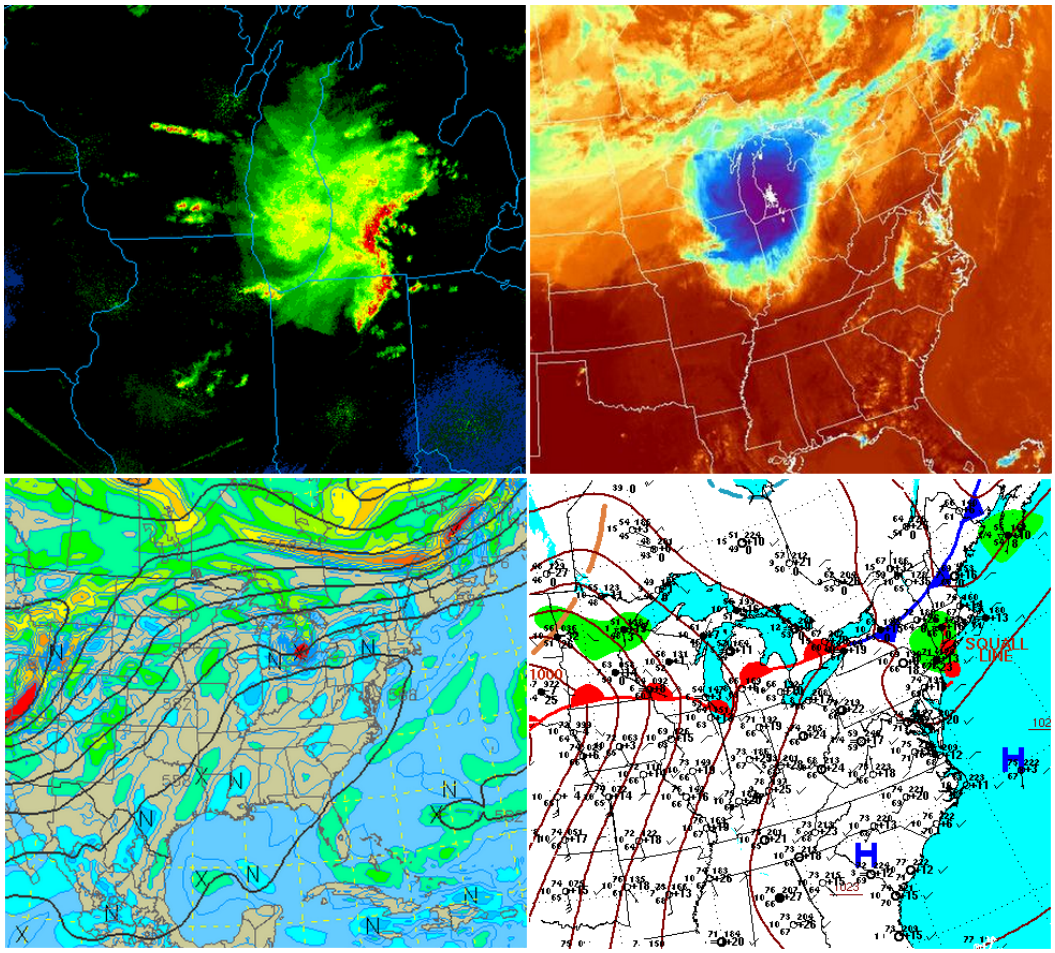

Figure 2: a) NEXRAD 1 km Mosaic at May 29, 2011 20Z, b) IR Satellite at May 29, 20:15Z, c) Vorticity at 500 mb at May 30, 0Z, d) Analyzed Surface Map at May 30, 12Z

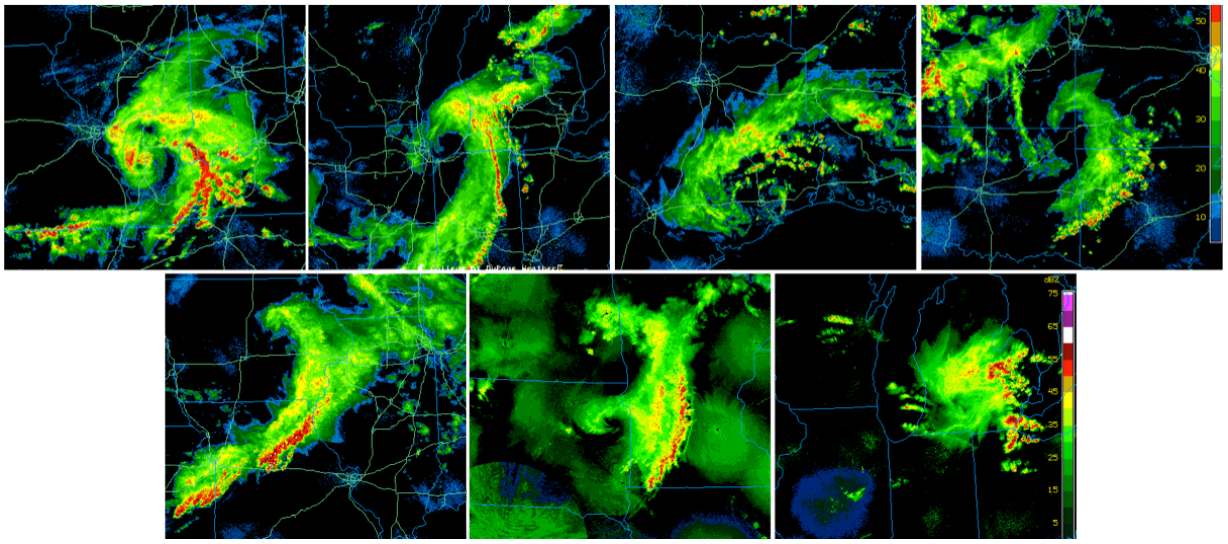

Figure 3: NEXRAD 1 km Mosaic of the seven selected MCVs, in order of left to right, top to bottom.

predilection for forming in those areas. Ultimately, seven cases were chosen; after this listing, they will be referred to as MCV01, MCV02, etc.

MCV01: May 8, 2009, Upper Mississippi Valley

MCV02: June 2, 2010, Iowa, Illinois, Michigan

MCV03: June 3, 2010, Texas

MCV04: June 7, 2010, Kansas, Missouri

MCV05: June 8, 2010, Nebraska, Iowa, Illinois

MCV06: May 9, 2011, North Dakota, Minnesota

MCV07: May 28-June 1, 2011, Midwest, Northeast, Florida

These cases all vary in intensity and longevity, with the shortest-lived being MCV06 at 11 hours and MCV07 being the longest-lived, at a whopping 5 and a half days. Once the cases were determined, RUC analyses data was used to verify the forecasts.

b. Plotting Real MCV Tracks

Once RUC data was obtained, it was separated case by case and accumulated into single event files. Grid Analysis and Display (GrADs) scripts provided by the advisor were then used to calculate and track and the MCV lifespan. The first script provided a map of absolute vorticity in the 400 mb to 700 mb layer across the domain, divided by hourly time steps beginning at 00Z. From this, the time of MCV initiation and dissipation could be determined, as well as overall track. The second script was then used to

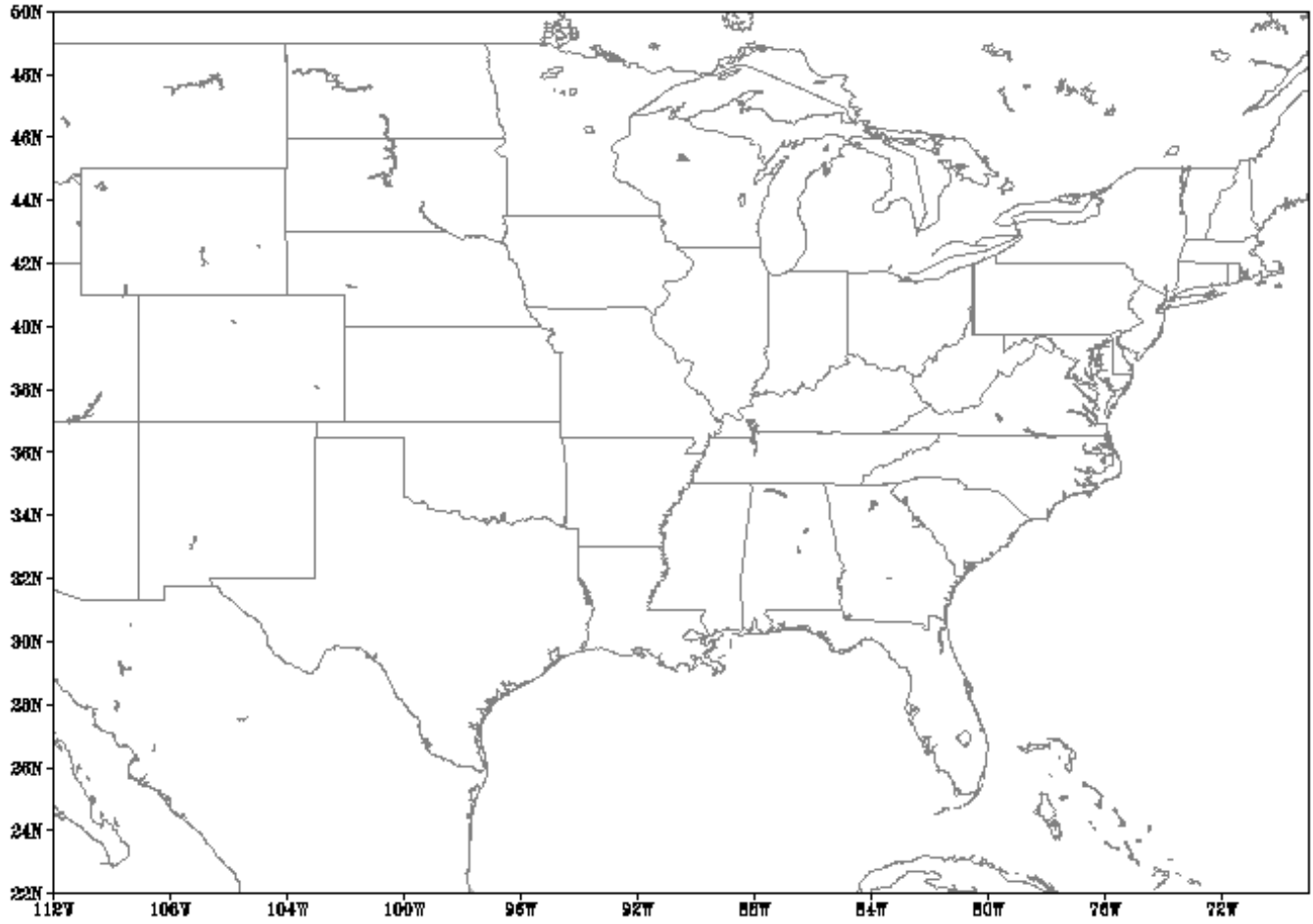

Figure 4: Map of the study's domain

subjectively pick out a rough estimate of the MCV's track length based on a composite of the absolute vorticity across the 400- 700 mb layer through the entire event. This track was then superimposed over a series of hourly time steps by script three, from which a more accurate and precise MCV path was found. This script output a text file containing the coordinates of the track, the time step, the average vorticity and maximum vorticity calculated at each time step. A fourth and final script then mapped this final track on a blank map of the domain.

For a swath of absolute vorticity to be considered an MCV, the absolute vorticity had to be greater or equal to $10^{-5}s^{-1}$, a boundary which was outlined by a thick black line in the provided GrADs scripts. Upon formation, the track followed the MCV until the vorticity fell below $10^{-5}s^{-1}$, and would

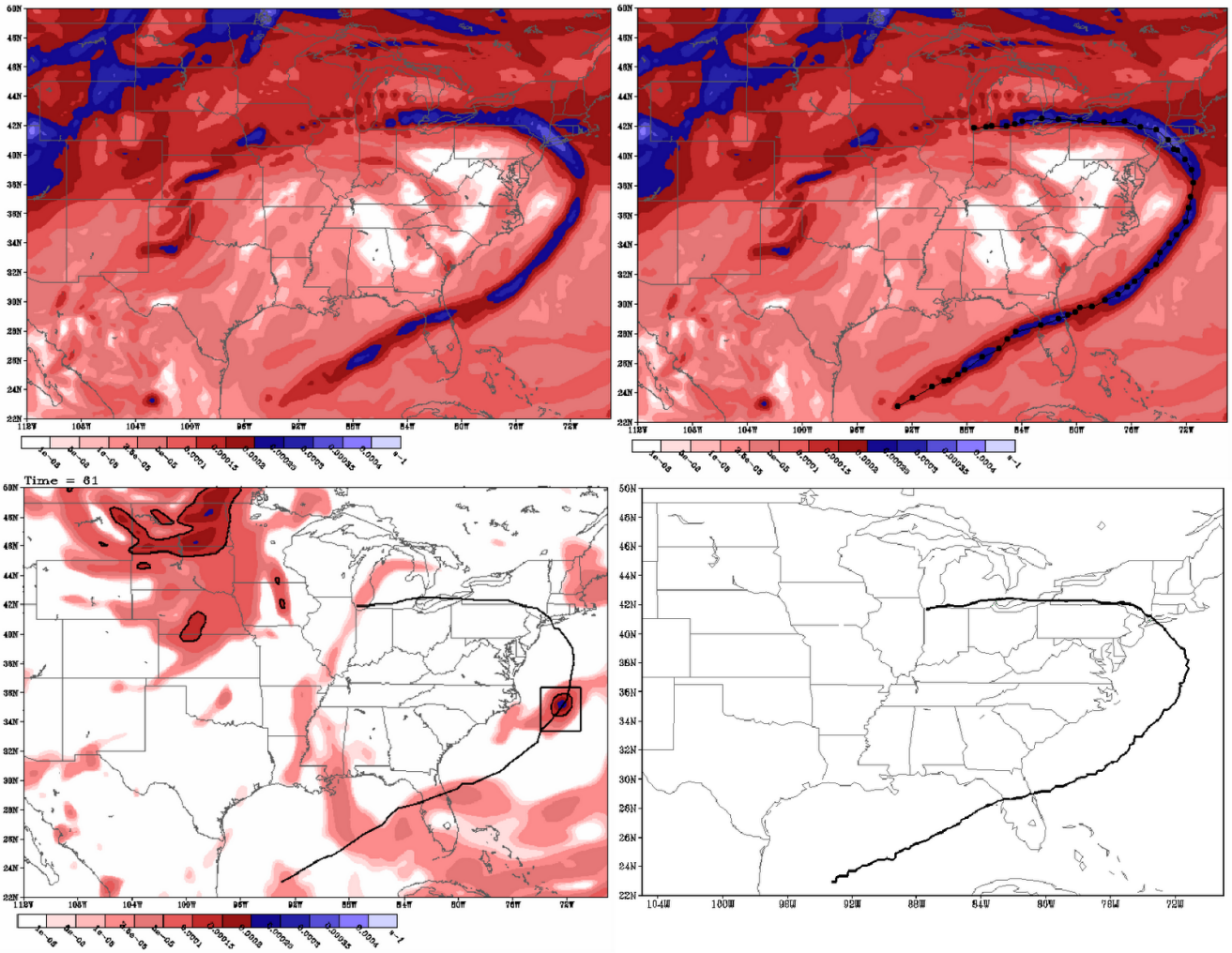

Figure 5: Clockwise From Top Left: Composite map of Absolute Vorticity / Preliminary Track overlaid on Absolute Vorticity Map / Preliminary Track on Map of Domain / Finalizing MCV Track

not continue the track should the storm reintensify. Furthermore, upon break-up of the vorticity maxima, the track followed the best-guess path based on radar and satellite data until dissipation. While it was found by Trier et al (2000a, 2000b) that secondary convection is a common occurrence, (observed in 9 of the 16 MCV cases Trier et al studied), this project made different assumptions: each MCV was treated as a single case that did not reintensify after initial dissipation, with any successive convection ignored in favor of high values of vorticity.

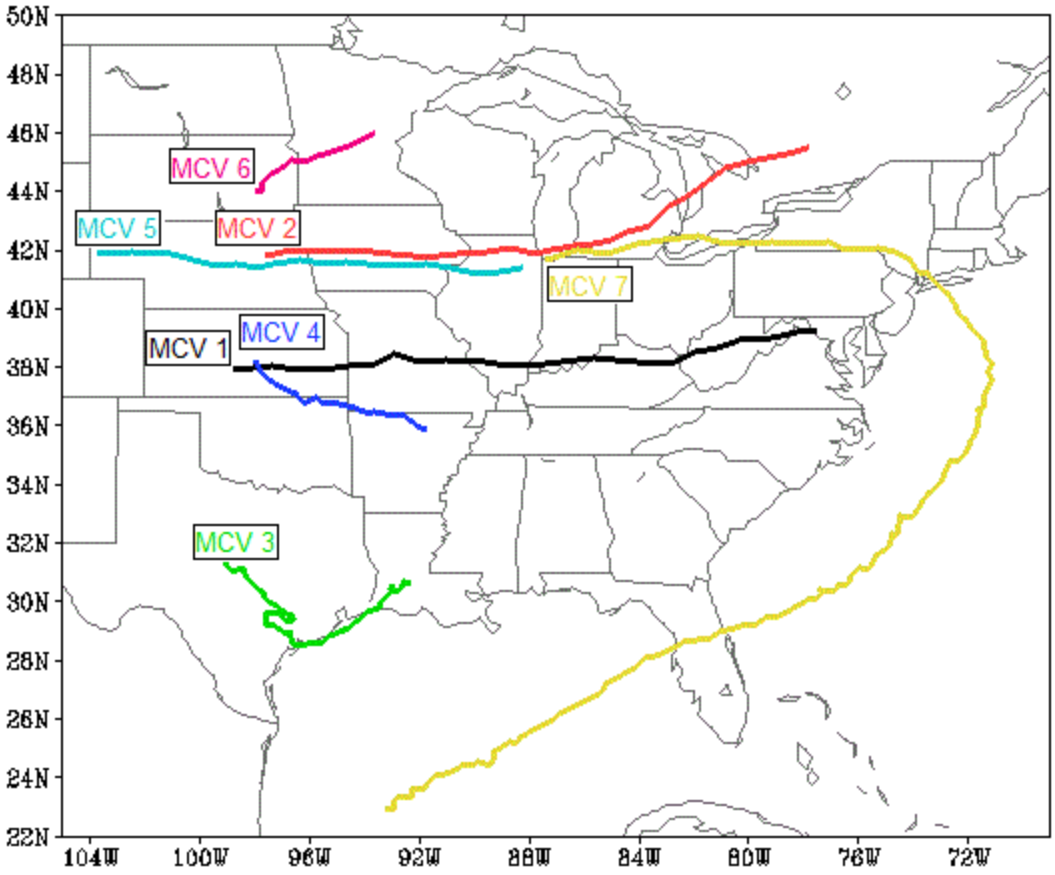

Figure 6: The final tracks of all MCVs events.

c. Plotting NAM and WRF Tracks

The same procedure performed on the RUC was used on corresponding data from the NAM and WRF, repeated through the models' successive forecasts, which were then grouped per MCV. Figures 7 and 8 show the general tracks as predicted by the NAM and the WRF vs the RUC, respectively.

d. Analysis of Data

Archived data were obtained from the Storm Prediction Center and the National Weather Service in order to understand the synoptic weather patterns that affected the MCVs from initiation onward. This data included upper level maps, surface maps, and precipitation maps, throughout the MCV's lifespan, from which notes on the formation and lifecycle of the MCV were obtained. A graphical spreadsheet program was used in conjunction with a program coded in python in order to run statistical analysis on

the accumulated data from the RUC, NAM, and WRF.

The python script utilized the text files output by the aforementioned GrADs script to compare RUC and NAM/WRF data. It generates distances between RUC and NAM/WRF coordinates per MCV case and the root mean square error for these distances, as well as for average and maximum vorticity.

3. Results

It is important to note that MCV07 proved to be an outlier in many aspects. As such, there were points in analysis that statistics had to be separated into two groups, one including the additional data of MCV07, and the other ignoring it.

On a synoptic scale, most of the MCVs formed in either the north or northeast quadrant of a longwave ridge, or in linear, baroclinic flow. These same features would also factor into the movements of the MCVs. Trier et al (2000a) found that of their sample size, most MCVs formed along or to the north of an east-west-oriented quasi-stationary front, in advance of a cold front, or without frontal association, instead initiating in baroclinic regions. These synoptic conditions for formation held true for most of this project's selected MCVs, with two events occurring in association with a cold front, one event forming alongside a quasi-stationary front, and two events having no such relations. However, two events created the need to add in one more zone of initialization.

MCV01 and MCV07 formed on the edge of an advancing warm front. These same two MCVs were also influenced by an upper level jet during the times of their formation, with both storms initiating in the right exit region of the jet. Both cases were somewhat extraordinary: MCV01 caused a severe weather outbreak in the mid-Mississippi River Valley, and MCV07 lived long enough to propagate into the Atlantic Ocean, turn south, and eventually become Invest 093 soon before impacting Florida. With only two examples of that particular synoptic background, it is impossible to determine with certainty that this was the reason for MCVs 01 and 07's extreme activity and longevity. To search for similar occurrences would be a fascinating future study.

MCVs also formed in areas that were around -10 degrees C to -14 degrees C at 300 mb, with only one exception, the weak MCV 6 at -18 degrees C at 300 mb, though it is again difficult to accurately determine anything more than a consistent pattern of events.

Three cases formed in the early morning hours (2am-6am) and four cases formed in the evening (5pm-10pm). These hours of formation are comparable to the climatological formation times (Markowski and Richardson 2010).

Not including MCV07, the average duration of the sample was 22.8 hours. Including MCV07, the duration increased to 34.7 hours. MCV06 proved to be the shortest lived of the bunch, lasting only 11 hours. In comparison, MCV07 lasted a total of 106 hours. This is an interesting contrast to the results of Trier et al (2000a), in which only 4 out of 16 recorded MCVs had a life surpassing 9 hours. The average maximum vorticity was $3.29432 * 10^{-4} s^{-1}$, with the most intense MCV being number 5 at $4.40663 * 10^{-4} s^{-1}$, and the weakest MCV being number 4 with $2.15572 * 10^{-4} s^{-1}$.

a. NAM Results

NAM tended to follow the climatological ideas of MCV formation times, keeping all but one of MCV initiation times between 10pm and 4am, with an average initiation time of 2:10 am.

The NAM forecasted an average duration of 21 and 22.6 hours, ignoring MCV07 and including MCV07 respectively. The NAM initialization forecast of the MCVs was within acceptable deviations, off by an average of 3 (±1) hours, generally forecasting the MCV to form earlier than actually observed. NAM forecasted dissipation depended strongly on the inclusion/removal of MCV07 from the average. Including MCV07 added an average of 12.5 (±1) hours to the MCVs' life spans. However, not considering MCV07 causes the average to shift to underforecasting by 7 (± 1) hours -- quite the gap. In this case, the latter average is probably more representative of the NAM's general performance, since MCVs with the duration and range of MCV07 are rare.

In terms of distance error, the NAM averaged at 276.34 km for initiation and 435.38 km for

dissipation, with no conclusive change over the past three years.. The model also tended to underestimate the intensity of the MCVs, with the maximum vorticity averaging at $2.53523 * 10^{-4} s{-}1$.

b. WRF Results

The WRF was variable in its forecasted initiation times, evenly split around the noontime hours and the 10pm -4am time range. The average time was 4:30am.

The WRF forecasted an average duration of 21 hours without MCV07 and an average duration of 73.25 hours with MCV07. For initiation, the WRF generally underestimated by 5.6 (± 1) hours. Dissipation, on the other hand, was overforecast drastically. The WRF consistently extended MCV lifespans by an average of 57.9 (± 1) hours without MCV07 and by 36.6 (± 1) hours with MCV07. The difference between including/removing MCV07 comes in this case from the WRF's underestimation of MCV07's formation at each forecast time.

The WRF forecasts had an average distance error of 310.91 km for initiation, and 742.94 km for dissipation. Due to the outlier MCV07, it's difficult to tell if there have been any conclusive changes over the past three years. However, it can be confidently said that the WRF typically overestimated the average maximum vorticity of the MCVs, with an average of $4.80782 * 10^{-4} s{-}1$

c. Comparisons

In time ranges of MCV initialization, the NAM followed the climatological formation time

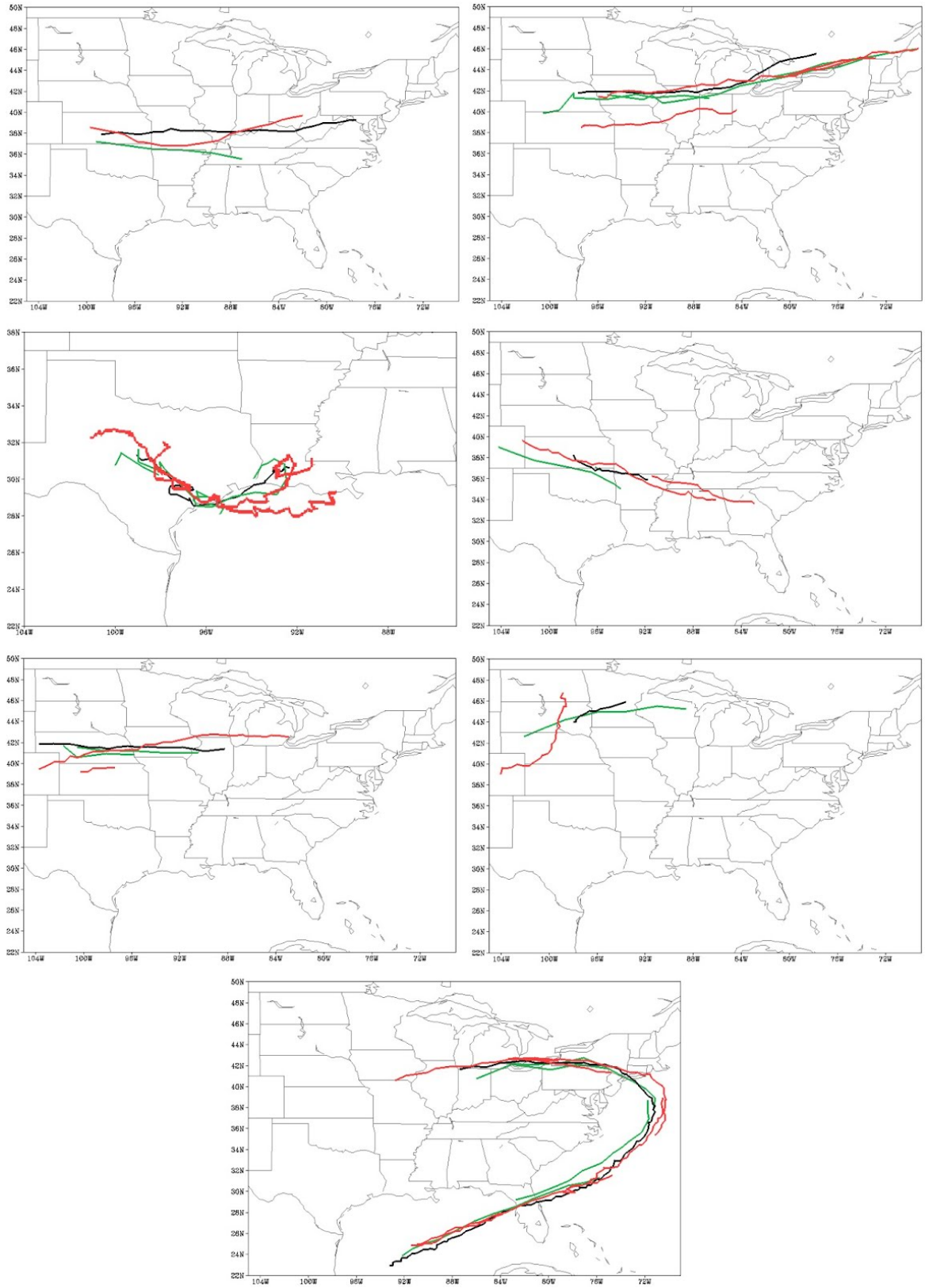

Figure 7: NAM (green) and WRF (red) forecasted paths superimposed over RUC path (black).

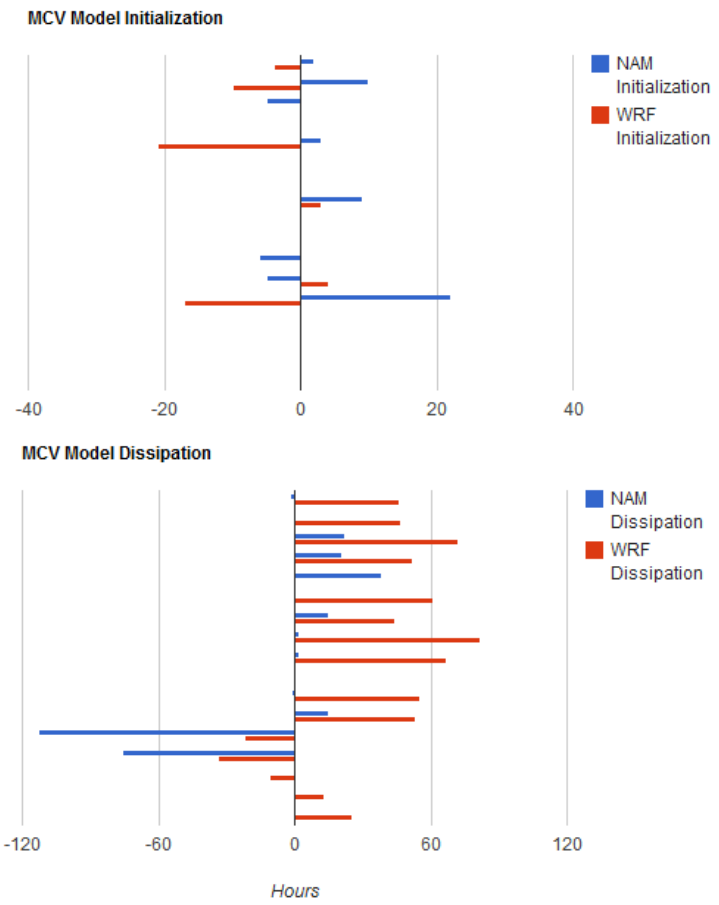

Figure 8: Comparison of the times (in hours) of initialization and dissipation between the NAM and WRF. The RUC is initialized at zero.

frame as put forth by Bartels and Maddox (1991) and other studies, namely the late evening and early morning hours, and was much more consistent with itself. In comparison, the WRF was much more variable, but actually closer to the actual MCV initialization hour than the NAM. However, the WRF was not as good as the NAM at keeping to the correct *dates* of initiation. In two cases, the WRF was missed initiation time by over 70 hours. In these cases, the tracks were calculated before the time disparity was realized. So for these instances, it was concluded that the WRF failed to forecast MCV formation entirely. The NAM, however, correctly forecasted MCV formation within 24 hours of actual initialization.

Of the two, the NAM remained closer to the actual lifespan of the MCV. In contrast, the WRF consistently extended the MCV duration by several days. Even so, the tracks remained similar to the RUC by propagating at a much slower rate.

Both models had similar distance errors in forecasting initiation points. Far more disparity in error exists with regards to dissipation. Of both, the NAM scored better with an average error of 432.38 km, while the WRF accumulated 742.95 km of error. In particular, the WRF forecasted MCV07 the worst, with over 2000 km of error. In comparison, the NAM was off by only 595.8 km. Naturally, both models forecasted more accurately after the MCV initiated.

The NAM typically underforecasted maximum vorticity, while the WRF overforecasted to an excessive degree. The NAM was typically within $1*10^{-4}s^{-1}$ of the actual vorticity while the WRF would increase the max vorticity by up to $5*10^{-4}s^{-1}$.

Using an R^2 value of .5 or higher to determine the strength of correlation, the NAM tended to correlate more precisely with the RUC data. Three out of the seven MCVs had average vorticity values with a strong, positive correlation to the RUC average vorticities. To determine statistical significance, a p-value of 0.05 was used.

The WRF was not as successful as the NAM when it came to predicting vorticity values for the MCVs. There was only one case (MCV07) where the WRF had a strong correlation to the RUC. Interestingly, this one case of strong, positive correlation was much stronger than any of the NAM cases; the WRF run had a nearly 1-to-1 relationship with the RUC data.

Davis et al (2003) makes mention of a possible connection between maximum vorticity and maximum possible longevity. This study finds no correlation between intensity and longevity directly with RUC, nor NAM, nor WRF, as shown in Figure 8. However, it is interesting to note that MCV07, with the greatest longevity, was not the strongest in terms of vorticity. This lack of correlation also rules out the cause of the WRF's long MCV durations being based on intensity, or vice versa. Similarly, there seems to be no correlation between intensity or duration and the time of MCV initiation.

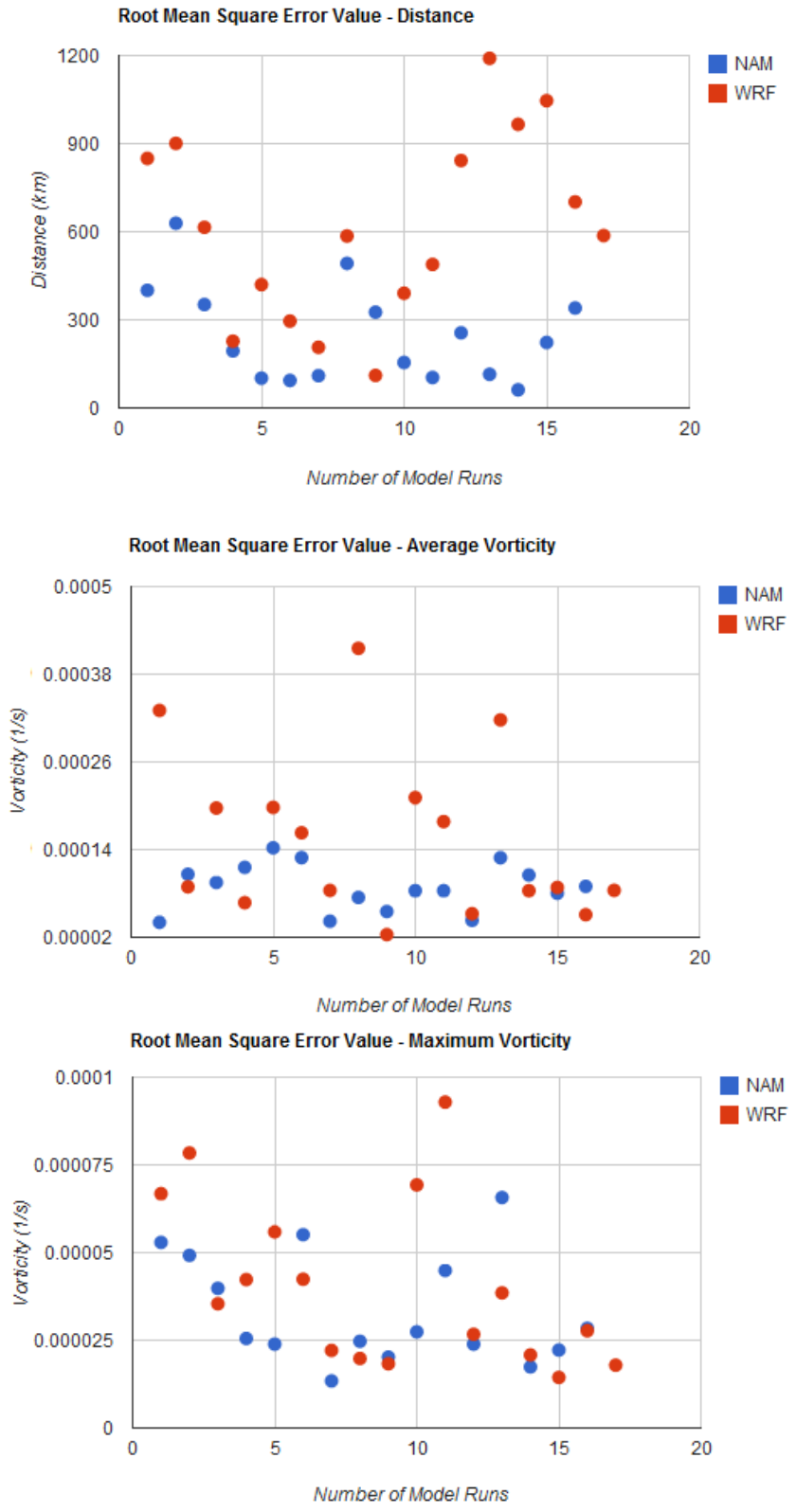

Figure 10: Root Mean Square Error Values between the NAM/WRF and RUC.

4. Conclusions

Both the NAM and the WRF are capable of predicting MCV formation for at least 24 hours in advance, a substantial lead time. However, neither model performs well in terms of MCV intensity or exact location.

In terms of lifespan of the MCVs, both the NAM and WRF show a tendency to extend the life of the MCV, with the WRF adding an average of over 48 hours and the NAM only adding 12. However, neither model shows substantial skill when it comes to the intensity of the MCVs, as both models regularly overestimated or underestimated the maximum vorticity, though the NAM was generally closer to the RUC data.

Location at MCV initiation can be as far off as several hundred kilometers, though both models become progressively worse at MCV dissipation, with one case showing error of 2000 km. The NAM again forecasts more accurately than the WRF.

Of the two models, the WRF has the most sporadic skill. It forecasts weaker MCVs with worse accuracy further from the initiation time. Even after initiation, essentially, the WRF was either spectacularly wrong or impressively right, with more instances of the former.

Of course, while the sample size is too small to make definite conclusions on the data, the results found do offer some clues as to the usefulness of the NAM and the WRF in forecasting for MCVs. Time restraints prevented the authors from completing all initial objectives.Further investigation is required to see how the results accomplished may be used to help improve the models' performances.

Acknowledgements

The authors would like to thank Adam Clark of NSSL/CIMMS for his help throughout the entire project.Thanks are also given to Andrew MacKenzie for his help in python code writing, as well as to the Storm Prediction Center, the National Weather Service, and the University Corporation for Atmospheric Research for use of their archived products.

REFERENCES:

Bartels, D. L., R. A. Maddox, 1991: Midlevel Cyclonic Vortices Generated by Mesoscale Convective Systems. Mon. Wea. Rev., 119, 104-118.

Clark, A. J., W. A. Gallus, M. Xue, and F. Kong, 2010: Convection-allowing and convection-parameterizing ensemble forecasts of a mesoscale convective vortex and associated severe weather environment. Wea. Forecasting, 25, 1052-1081.

Coniglio, M. C., S. F. Corfidi, and J. S. Kain, 2011: Environment and early evolution of the 8 May 2009 derecho-producing convective system. Mon. Wea. Rev., 139, 1083-1102.

Davis, Christopher A., D. A. Ahijevych, S. B. Trier, 2003: Detection and Prediction of Warm Season mid-tropospheric Vortices by the Rapid Update Cycle. Mon. Wea. Rev., 130, 24–42.

Hertenstein, R. F. A., and W. H. Schubert, 1991: Potential vorticity anomalies associated with squall lines. Mon. Wea. Rev, 119, 1663–1672

Kong, F., K. K. Droegemeier, and N. L. Hickmon, 2007a: Multi-resolution ensemble forecasts of an observed tornadic thunderstorm system. Part II. Storm- scale experiments. Mon. Wea. Rev., 135, 759–782

Markowski, P., and Y. Richardson, 2010: Mesoscale Meteorology in Midlatitudes. Wiley-Blackwell, 265-273.

Raymond and Jiang, 1990: A theory for long-lived mesoscale convective systems. J. Atmos. Sci., 51, 1352-1371.

Snook, N., Z. Ming, and Y. Jung, 2011: Analysis of a Tornadic Mesoscale Convective Vortex Based on Ensemble Kalman Filter Assimilation of CASA X-Band and WSR-88D Radar Data. Mon. Wea. Rev., 139, 3446-3468.

Trier, S.B., C.A. Davis, and J.D. Tuttle, 2000: Long-Lived Mesoconvective Vortices and Their Environment. Part I: Observations from the Central United States during the 1998 Warm Season. Mon. Wea. Rev., 128, 3376-3395

Trier, S.B., C.A. Davis, and W.C. Skamarock, 2000: Long-Lived Mesoconvective Vortices and Their Environment. Part II: Induced Thermodynamic Destabilization in Idealized Simulations. Mon. Wea. Rev., 128, 3396-3412

Zhang, F., A. M. Odins, and J. W. Nielsen-Gammon, 2006: Meso-scale predictability of an extreme warm-season precipitation event. Wea. Forecasting, 21, 149–166.